Driven Andreev molecule

Andriani Keliri* and Benoît Douçot
Laboratoire de Physique Théorique et Hautes Energies, Sorbonne Université and CNRS UMR 7589, 4 place Jussieu, 75252 Paris Cedex 05, France

(Received 14 October 2022; revised 7 February 2023; accepted 13 February 2023; published 6 March 2023)

We study the voltage-biased S-QD-S-QD-S Josephson junction, composed of three superconductors (S) and two quantum dots (QDs). In the absence of an applied voltage, the Andreev bound states on each quantum dot hybridize, forming an "Andreev molecule." However, understanding of this system in a nonequilibrium setup is lacking. Applying commensurate dc voltages on the bijunction makes the system time periodic, and the equilibrium Andreev bound states evolve into a ladder of resonances with a finite lifetime due to multiple Andreev reflections (MARs). Starting from the time-periodic Bogoliubov–de Gennes equations we map the problem to a tight-binding chain in Floquet space. The resolvent of this non-Hermitian block matrix is obtained via a continued fraction method. We numerically calculate the Floquet-Andreev spectra which could be probed by local tunneling spectroscopy on the dots. We also consider the subgap current, and show that the Floquet resonances determine the position of the MAR steps. Proximity of the two dots causes splitting of the steps, while at large distances we observe interference effects which cause oscillations in the current-voltage curves. The latter effect should persist at very long distances.

DOI: 10.1103/PhysRevB.107.094505

I. INTRODUCTION

At its heart, superconductivity has the distinct characteristic of a coherent macroscopic quantum state. Together with that other particularly quantum phenomenon—magnetism—superconductivity is bound to be an essential element for quantum computing applications [1]. The working principle of such superconducting circuits is the Josephson effect(s) [2,3]. A more microscopic description of Josephson junctions reveals the Andreev reflection mechanism and the resulting Andreev bound states (ABSs) as responsible for carrying most of the Josephson current across a phase-biased junction. Apart from using the ABSs to realize an "Andreev qubit" [4–7], other, more complex geometries are being explored. Multiterminal Josephson junctions are drawing particular interest since, on the one hand, they could be an alternative way to engineer topological states, even when the junctions are made from topologically trivial materials [8,9], and on the other, they can be used to create correlations among pairs of Cooper pairs, the so-called quartets [10–13].

In an analogy to the formation of a molecule, bringing two ABSs carrying junctions close enough should result in a hybridization of the ABS wave functions [14,15]. The hybridization would create nonlocal effects in the current, whereby changing the phase on one junction would change the current flowing through the other. This could be useful for realizing qubits whose coupling, for example, can be tuned by changing their phase difference, but one should have a distance of the junctions which remains comparable to the superconducting coherence length ξ_0. In a typical superconductor, such as aluminum, $\xi_0 \sim 100$ nm. The first experiments realizing Andreev molecules and measuring nonlocal effects in the Josephson current have already been performed on semiconducting nanowires [16,17]. However, such systems host subgap states which are different from the ABS (the Yu-Shiba-Rusinov states) because they are in the opposite limit of strong Coulomb interaction ($U > \Delta$). Another interesting proposal is to use an Andreev molecule as an elementary unit for realizing a physical Kitaev chain, which could host the elusive Majorana state [18,19].

Meanwhile, there is increasing interest in periodically driven (Floquet) systems since the external drive can be used to engineer new "hidden" states and dynamically control properties otherwise inaccessible in equilibrium [20–23], for example, to open band gaps in graphene [24], or induce edge states that carry an anomalous Hall current [25]. Moreover, Floquet qubits would offer numerous optimal working points to choose from by changing the driving parameters [26–28], contrary to their static counterparts whose parameters are mostly tuned during fabrication. Experimentally, the realization of Floquet states is often difficult due to thermalization [29] and short lifetimes. Nevertheless, a recent experiment has reported the generation of long-lived steady Floquet-Andreev states realized by continuous microwave irradiation of a graphene Josephson junction [30].

Periodic driving of a superconducting junction could also be realized by voltage-biasing the junction. It has been known since the 1980s that, in such cases, multiple Andreev reflections (MARs) of quasiparticles between the junctions' superconductors lead to a subharmonic gap structure of the current-voltage characteristics: the current exhibits jumps at particular voltage values which are integer subdivisions of the superconducting gap $eV = 2\Delta/n$ [31,32]. In the limit of resonant tunneling through the junction the subgap structure is greatly modified [33–36]: features

*akeliri@lpthe.jussieu.fr

corresponding to an odd number of MARs are enhanced, while even trajectories are suppressed. In the driven case one may, moreover, wonder at the fate of the subgap bound states. Previous work has shown that instead of the equilibrium ABS one obtains ladders of resonances separated in energy by multiples of the basic frequency of the drive [37,38]. This is analogous to the formation of Wannier-Stark ladders in a solid under an electric field [39,40]. The resonances have a finite width since MARs provide a mechanism of coupling of the once discrete states (ABSs) to the continuum of states of the reservoirs. Nevertheless, the lifetime of the Floquet states can still be very long, since MARs are higher-order processes which at small voltage give an exponentially small width in Δ/eV [38].

In this work, we study the Floquet spectrum of a driven Andreev molecule, in the limit of resonant tunneling through the junctions. We therefore model each junction as a noninteracting resonant level (a quantum dot) coupled to superconducting leads. The problem can be mapped to a tight-binding chain in Floquet space. We take advantage of this tight-binding structure to derive the Green's function on the dot(s) iteratively. We find that the equilibrium discrete states on each dot are dressed by MAR processes and evolve into ladders of resonances, as expected. The spectrum of the driven molecule exhibits level splitting when the separation between the dots is comparable to the superconducting coherence length, $R \sim \xi_0$. These Floquet-Andreev resonances should leave their trace in the dc current. We therefore calculate the steady-state current passing through one junction and see that the proximity of the second junction modifies the usual MAR steps, which accordingly exhibit splitting into substeps. Moreover, when the two junctions are separated by a large distance $R \gg \xi_0$, we find oscillations of the spectral functions above the gap and, consequently, of the current-voltage (I-V) curves. This phenomenon is akin to the Tomasch effect [41,42], and is due to long-distance correlations mediated by propagating quasiparticles in the middle superconductor, as has been discussed in recent work [43]. Indeed, we find that the spectral function at a fixed voltage value is an oscillatory function of a Tomasch phase factor. This Floquet-Tomasch effect should persist at distances which are up to two orders of magnitude larger than the superconducting coherence length, as in the Tomasch experiment.

The rest of this paper has the following structure. In Sec. II we define the model Hamiltonian and derive the Floquet-Lippmann-Schwinger (FLS) equations. We then show how to calculate the resolvent operator and the subgap current. Section III presents our numerical results for the Floquet spectra. Section IV shows our results for the subgap current, first for the current through a single junction, and then for the Andreev molecule. Conclusions and perspectives are provided in Sec. V. We show that the spectral function oscillates due to a Tomasch phase factor in the Appendix.

II. MODEL AND METHOD

A. Hamiltonian

The system considered here is the three-terminal Josephson junction, with two quantum dots each connected to a superconducting reservoir S_a, S_b, and both connected to a central superconducting reservoir S_c, as illustrated in Fig. 1. We study the simplest case where each dot is modeled by a single discrete resonant level at energy $\epsilon_d = 0$. Some additional plots are provided in the Supplemental Material [44] for the case of nonresonant dots.

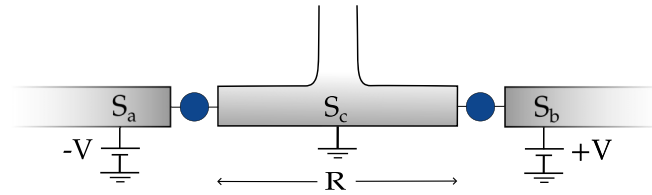

FIG. 1. Schematic representation of the three-terminal Josephson junction setup considered in this paper. The two quantum dots host a single discrete level at zero energy and are separated through the middle superconducting reservoir S_c by a distance R. The reservoirs are considered to be one dimensional and are voltage biased along the quartet line: $(V_a, V_c, V_b) = (-V, 0, +V)$.

When a dc voltage V is applied across a superconducting junction, its Hamiltonian acquires a time-periodic dependence according to the Josephson relation $\phi(t) = \phi(0) + \frac{2eV}{\hbar}t$, where ϕ is the superconducting phase difference across the junction. In this paper, we use the so-called quartet configuration when biasing the superconducting reservoirs: $(V_a, V_c, V_b) = (-V, 0, +V)$. This choice simplifies the problem since it leads to a single basic frequency $\omega_0 = eV/\hbar$ for the whole system. The resulting Hamiltonian has the discrete symmetry $\mathcal{H}(t) = \mathcal{H}(t + T)$, where $T = \frac{2\pi}{\omega_0}$ is the period of the drive. A simple gauge transformation then permits to write the Hamiltonian in the form

$$\mathcal{H}(t) = \mathcal{H}_0 + \mathcal{V}(t). \tag{1}$$

The static part $\mathcal{H}_0$ is a sum of the BCS Hamiltonians describing the superconducting reservoirs:

$$\mathcal{H}_0 = \sum_{jk\sigma} \epsilon_k c^\dagger_{jk\sigma} c_{jk\sigma} + \sum_{jk} (\Delta_j c^\dagger_{jk\uparrow} c^\dagger_{j-k\downarrow} + \Delta^*_j c_{j-k\downarrow} c_{jk\uparrow}). \tag{2}$$

The operators $c^\dagger_{jk\sigma}$ and $c_{jk\sigma}$ create and annihilate an electron in the j reservoir with momentum k and spin σ. We use the notation $\Delta_j = \Delta e^{i\phi_j}$, and consider that all superconductors have a gap of equal magnitude.

The time-periodic part $\mathcal{V}(t)$ describes the tunneling between the dots labeled by $i = \{1, 2\}$ and the reservoirs labeled by $j = \{a, b, c\}$:

$$\mathcal{V}(t) = \sum_{i\in \text{dots}} \sum_{jk\sigma} \left(J_j(x_i) e^{is_j\omega_0 t} d^\dagger_{i\sigma} c_{jk\sigma} + J^\star_j(x_i) e^{-is_j\omega_0 t} c^\dagger_{jk\sigma} d_{i\sigma} \right). \tag{3}$$

For convenience, we take the dots' positions to be at $x_1 = 0$, $x_2 = R$, and the tunnel couplings to be $J_j(x_i) = J_j e^{ikx_i}$, with a real amplitude $J_j = J^\star_j$. We have moreover used the notation $V_j = s_j V$.

The main idea is to exploit the symmetry of the Hamiltonian by looking for time-periodic (Floquet) solutions to the Bogoliubov–de Gennes (BdG) equations. The problem can then be mapped to an effective tight-binding model with sites labeled by the Floquet harmonics [45–48]. Time then no

longer appears in the equations, but is traded for a fictitious Floquet direction. In such time-periodic systems the energy is not a well-defined quantity [49–51], but is defined modulo the frequency of the drive. We therefore talk of "quasienergies" of the system, in direct analogy to the quasimomenta of Bloch theory due to periodicity in space. In our study, the choice of the quartet configuration leads to a mapping to an effective one-dimensional Floquet chain. The method described can be however applied to any set of commensurate voltages. In the case of incommensurate voltages, one will obtain an N-dimensional Floquet lattice instead, where N is the number of incommensurate drive frequencies [52].

B. Floquet-Lippmann-Schwinger equations

In the absence of tunneling, $\mathcal{V}(t) = 0$, the BdG equation can be written as

$$i\frac{d}{dt}\gamma^\dagger_{lk\sigma} = \left[\mathcal{H}_0, \gamma^\dagger_{lk\sigma}\right] = E_{lk}\gamma^\dagger_{lk\sigma}. \tag{4}$$

The bare quasiparticle operator $\gamma_{lk\sigma}$ is an eigenstate of the superconducting reservoir labeled $l = \{a, b, c\}$:

$$\gamma^\dagger_{lk\sigma}(t) = e^{-iE_{lk}t}\left(x_{lk}e^{i\phi_l/2}c^\dagger_{lk\sigma} + \sigma y_{lk}e^{-i\phi_l/2}c_{l-k-\sigma}\right), \tag{5}$$

and the coefficients x, y are the usual coefficients obtained by diagonalizing the BCS Hamiltonian [53],

$$x^2_{lk} = \frac{E_{lk} + \epsilon_k}{2E_{lk}} \quad \text{and} \quad y^2_{lk} = \frac{E_{lk} - \epsilon_k}{2E_{lk}}, \tag{6}$$

with $E_{lk} \equiv \sqrt{\epsilon_k^2 + |\Delta_l|^2}$ the excitation energy needed for adding an electron or a hole to the BCS ground state.

When the tunneling is turned on, the discrete ABSs on the dots become resonances due to the MAR processes which connect them to the superconducting continua. We can then use the Lippmann-Schwinger method from quantum scattering theory to construct dressed operators Γ which tend to the bare quasiparticle operators γ at the limit of zero tunnel couplings. We therefore introduce a dressed quasiparticle operator $\Gamma^\dagger_{lk\sigma}$ describing a quasiparticle being injected from a source reservoir l with momentum k and spin σ, to any of the reservoirs j, and quantum dot(s) i:

$$\Gamma^\dagger_{lk\sigma}(t) = \gamma^\dagger_{lk\sigma}(t) + e^{-iE_{lk}t}\sum_{m\in\mathbb{Z}} e^{-im\omega_0 t} \times \left[\sum_{i\in\text{dots}}\left(u_m(i;lk)d^\dagger_{i\sigma} + \sigma v_m(i;lk)d_{i-\sigma}\right) + \sum_{jk'}\left(U_m(jk';lk)c^\dagger_{jk'\sigma} + \sigma V_m(jk';lk)c_{j-k'-\sigma}\right)\right]. \tag{7}$$

The amplitudes $u_m(i;lk), v_m(i;lk)$ have respectively the meaning of an electron- or holelike amplitude on the dot i, corresponding to a Floquet harmonic with quasienergy $E_{lk} + m\omega_0$, while capital letters U_m, V_m correspond to amplitudes in the reservoirs.

The dressed operators are Floquet solutions of the BdG equations:

$$i\frac{d}{dt}\Gamma^\dagger_{lk\sigma}(t) = \left[\mathcal{H}(t), \Gamma^\dagger_{lk\sigma}\right], \tag{8}$$

and therefore obey the Floquet theorem,

$$\Gamma^\dagger(t+T) = e^{-iE_{lk}t}\Gamma^\dagger(t). \tag{9}$$

We use the ansatz of Eq. (7) and substitute into Eq. (8). After integrating out the amplitudes of the reservoirs, we are led to the following set of inhomogeneous Lippmann-Schwinger equations for the amplitudes on the dots:

$$\begin{aligned}
&(E_{lk} + m\omega_0 + i\eta)u_m(i;lk) - \sum_{ji'}\left[g^{11}_{j,ii'}(m+s_j)u_m(i';lk) + g^{12}_{j,ii'}(m+s_j)v_{m+2s_j}(i';lk)\right] = \delta_{m,-s_l}J_l(x_i)x_{lk}e^{i\phi_l/2},\\
&(E_{lk} + m\omega_0 + i\eta)v_m(i;lk) - \sum_{ji'}\left[g^{21}_{j,ii'}(m-s_j)u_{m-2s_j}(i';lk) + g^{22}_{j,ii'}(m-s_j)v_m(i';lk)\right] = -\delta_{m,s_l}J_l(x_i)y_{lk}e^{-i\phi_l/2}.
\end{aligned} \tag{10}$$

In the above equation, $g_{j,ii'}\delta_{ii'} \equiv g_j$ is the Green's function for the j superconducting reservoir, defined as

$$g_j(\omega) = \frac{\Gamma_j}{iv_F q(\omega)}\begin{pmatrix}\omega & -\Delta_j\\ -\Delta_j^* & \omega\end{pmatrix}, \quad \text{and} \quad v_F q(\omega) \equiv i\sqrt{\Delta^2 - \omega^2}\theta(\Delta - |\omega|) + \text{sign}(\omega)\sqrt{\omega^2 - \Delta^2}\theta(|\omega| - \Delta). \tag{11}$$

We have used the notation $\Gamma_j = \pi\rho_0 J_j^2$, where ρ_0 is the density of states in the normal state of the superconductors. Moreover, since the quasienergy appears in the combination $\omega + m\omega_0$, it is convenient to use the shorthand $f(m)$ instead of $f(\omega + m\omega_0)$, for any function f.

The nondiagonal part which couples the amplitudes on different dots $g_{j,ii'}(m)(1 - \delta_{ii'}) \equiv g_j(m, R)$ is a nonlocal Green's function and depends explicitly on the distance between the two dots:

$$g_j(m, R) = e^{iq(m)R}[\cos(k_F R)g_j(m) + \sin(k_F R)\Gamma_j\sigma_z], \tag{12}$$

where k_F is the Fermi wave vector. The reservoirs have been chosen as one dimensional (1D) for simplicity, but this should not influence the qualitative description. In equilibrium, a more careful analysis of the effect of dimensionality [54] and comparison with Ref. [14] shows that if the propagation in the middle reservoir is three dimensional (3D) instead of 1D, then the resulting hybridization of the Andreev molecule will be smaller at a given distance by an order of magnitude [55]. Moreover, we consider that the middle superconductor S_c is large on the mesoscopic scale, so that it can have a well-defined electrochemical potential, but that the distance R between the two dots remains finite.

The nonlocal Green's function mediates the coupling between the junctions and oscillates on two very different length scales. For energies smaller than the gap, $|\omega| < \Delta$, the factor $e^{iqR} = e^{-\sqrt{1-(\omega/\Delta)^2}R/\xi_0}$ decays exponentially over distances larger than the superconducting coherence length $\xi_0 \equiv v_F/\Delta$, while for energies above the gap e^{iqR} oscillates without decay. These nonvanishing oscillations physically represent quasiparticle propagation in the continuum of the reservoirs, which is therefore not bound by the superconducting coherence length. On the other hand, the phase $k_F R$ oscillates rapidly at the scale of the Fermi wavelength $\lambda_F = 2\pi/k_F$, since the superconducting coherence length is typically much larger than the Fermi wavelength, $\xi_0 \simeq 10^3 \lambda_F$. The former length scale is coupled with the quasiparticle energy ω, while the latter would give a geometric effect. Since the two scales are very different, and we want to focus on new physics related to the energy dependence rather than to any geometric effects, we will assume that the phase $k_F R$ is fixed. We discuss this choice in some more detail in the Supplemental Material [44].

Introducing the Nambu spinor

$$\Psi_m = (u_m(1), v_m(1), u_m(2), v_m(2))^T$$

which collects the amplitudes on the two dots, we can rewrite Eq. (10) by defining a linear operator $\mathcal{L}$ which acts on the states Ψ_m in the following way:

$$(\mathcal{L}\Psi)_m \equiv M_m^0 \Psi_m - M_{m+1}^+ \Psi_{m+2} - M_{m-1}^- \Psi_{m-2} = S_m. \quad (13)$$

Equation (13) is the Floquet chain advertised above. In the tight-binding analogy, the matrix M_m^0 describes a self-energy at position m of the chain, while matrices $M_{m\pm1}^{\pm}$ describe "hopping" to neighboring sites $m \pm 2$. The fact that m couples to $m \pm 2$ is a consequence of coupling via second-order Andreev reflection processes. Explicitly, the matrix M^0,

$$M_m^0 = E_m \mathbb{1}_4 - \begin{pmatrix} \Sigma_1(m) & g_c(m,R) \\ g_c(m,R) & \Sigma_2(m) \end{pmatrix}, \quad (14)$$

contains a nonlocal coupling of the two dots through the Green's function of the middle superconductor $g_c(m,R)$, and local Andreev reflection terms on each of the dots, collected in the block diagonal in the $\Sigma_{1,2}$ matrices:

$$\Sigma_1(m) = g_c(m) + \begin{pmatrix} g_a^{11}(m-1) & 0 \\ 0 & g_a^{22}(m+1) \end{pmatrix},$$
$$\Sigma_2(m) = g_c(m) + \begin{pmatrix} g_b^{11}(m+1) & 0 \\ 0 & g_b^{22}(m-1) \end{pmatrix}. \quad (15)$$

The matrices $M^{\pm}$ are

$$M_m^- = \begin{pmatrix} 0 & g_a^{12}(m) & 0 & 0 \\ 0 & 0 & 0 & 0 \\ 0 & 0 & 0 & 0 \\ 0 & 0 & g_b^{21}(m) & 0 \end{pmatrix},$$
$$M_m^+ = \begin{pmatrix} 0 & 0 & 0 & 0 \\ g_a^{21}(m) & 0 & 0 & 0 \\ 0 & 0 & 0 & g_b^{12}(m) \\ 0 & 0 & 0 & 0 \end{pmatrix}. \quad (16)$$

Remark. Equation (10) is an inhomogeneous equation because of the source terms on the right-hand side, collected in the column matrix S_m. In the following sections we are interested in the spectrum on the dots. We can then simply consider the homogeneous version of Eq. (10), since it is sufficient to find the resonances of the operator $\mathcal{L}$. In later sections, however, we will be interested in the transport properties (current). Then, we will have to restore the source term.

C. Iterative construction of the resolvent operator

If the resolvent operator $\mathcal{R}$ is the inverse of the operator $\mathcal{L}$, then knowledge of $\mathcal{R}$ allows straightforward calculation of the amplitudes on the dots:

$$u_m(i;lk) = \sum_{i'} \left[\mathcal{R}_{m,-s_l}^{e_i e_{i'}} J_l(x_{i'}) x_{lk} e^{i\phi_l/2} - \mathcal{R}_{m,s_l}^{e_i h_{i'}} J_l(x_{i'}) y_{lk} e^{-i\phi_l/2} \right],$$
$$v_m(i;lk) = \sum_{i'} \left[\mathcal{R}_{m,-s_l}^{h_i e_{i'}} J_l(x_{i'}) x_{lk} e^{i\phi_l/2} - \mathcal{R}_{m,s_l}^{h_i h_{i'}} J_l(x_{i'}) y_{lk} e^{-i\phi_l/2} \right]. \quad (17)$$

Finding the poles of the resolvent operator corresponds to finding the spectrum of the operator $\mathcal{L}$. The resolvent $\mathcal{R}$ is an operator which lives in the extended dot $\otimes$ Nambu $\otimes$ Floquet space. Upper indices correspond to the combined dot $\otimes$ Nambu space, and lower indices correspond to the infinite Floquet space. The inhomogeneous FLS equations for the resolvent elements are

$$M_m^0 \mathcal{R}_{mn} - M_{m+1}^+ \mathcal{R}_{m+2,n} - M_{m-1}^- \mathcal{R}_{m-2,n} = \delta_{mn} \mathbb{1}. \quad (18)$$

For a tridiagonal block-matrix Hamiltonian, such as the one we are dealing with, it follows generally that its resolvent can be written in continued fraction form [56,57]. The continued fraction representation is equivalent to the usual Dyson equation [58].

Starting from Eq. (18) it is straightforward to construct the resolvent elements by iteration, assuming a source at some index n and a cutoff at some large Floquet index $\pm N$, with $|N| \geqslant \frac{\Delta}{\omega_0}$. The latter is equivalent to assuming that the wave function on the dot decays exponentially at energies above the gap $|\omega + N\omega_0| \gg \Delta$. Physically, the first values of m will correspond to multiple quasiparticle reflection processes, by which the quasiparticle gains energy equal to $m\omega_0$. When m is large enough so that $\omega + m\omega_0 > \Delta$, the quasiparticle enters the superconducting continuum, thus macroscopically resulting in a dissipative quasiparticle flow with normal conductance values. The smaller the voltage value, the more Floquet harmonics we need to take into account. We have the following system consisting of $2N+1$ equations:

$$\begin{aligned}
&M_{-N}^0 \mathcal{R}_{-N,n} - M_{-N+1}^+ \mathcal{R}_{-N+2,n} - \cancel{M_{-N-1}^- \mathcal{R}_{-N-2,n}} = 0 \\
&\vdots \\
&M_{n-2}^0 \mathcal{R}_{n-2,n} - M_{n-1}^+ \mathcal{R}_{nn} - M_{n-3}^- \mathcal{R}_{n-4,n} = 0 \\
&M_n^0 \mathcal{R}_{nn} - M_{n+1}^+ \mathcal{R}_{n+2,n} - M_{n-1}^- \mathcal{R}_{n-2,n} = \mathbb{1} \\
&M_{n+2}^0 \mathcal{R}_{n+2,n} - M_{n+3}^+ \mathcal{R}_{n+4,n} - M_{n+1}^- \mathcal{R}_{nn} = 0 \\
&\vdots \\
&M_N^0 \mathcal{R}_{Nn} - \cancel{M_{N+1}^+ \mathcal{R}_{N+2,n}} - M_{N-1}^- \mathcal{R}_{N-2,n} = 0
\end{aligned} \quad (19)$$

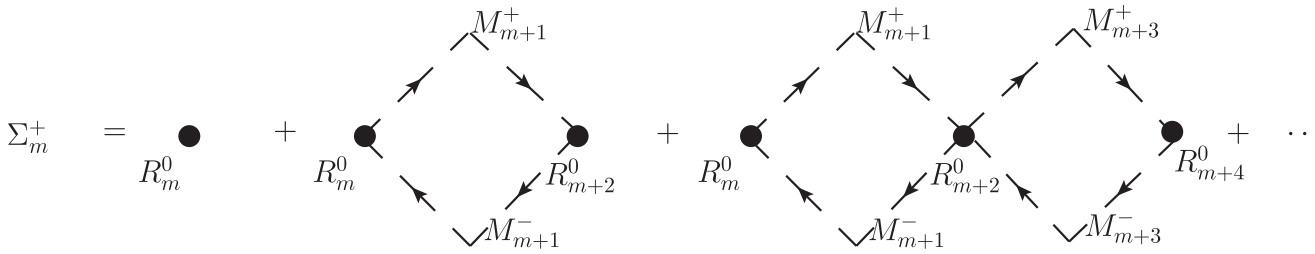

FIG. 2. Diagrammatic representation of the forward-scattering self-energy. Σ_m^+ resums loops to the right of site m.

We solve this system of equations by iteration, and find that the diagonal elements are resummed into a geometric series

$$\mathcal{R}_{mm} = \left[M_m^0 - M_{m+1}^+ \Sigma_{m+2}^+ M_{m+1}^- - M_{m-1}^- \Sigma_{m-2}^- M_{m-1}^+\right]^{-1} \tag{20}$$

with forward and backward self-energy matrices, $\Sigma^{\pm}$, that can be calculated recursively once boundary conditions are imposed, that is, once $\Sigma_{\pm N}^{\pm}$ is set to zero at some large number $\pm N$. We find that

$$\begin{aligned}\Sigma_m^+ &= \frac{1}{M_m^0 - M_{m+1}^+ \Sigma_{m+2}^+ M_{m+1}^-},\\ \Sigma_m^- &= \frac{1}{M_m^0 - M_{m-1}^- \Sigma_{m-2}^- M_{m-1}^+}.\end{aligned} \tag{21}$$

The nondiagonal resolvent elements $\mathcal{R}_{mn}$ can then be expressed using the self-energy matrices

$$\begin{aligned}\mathcal{R}_{mn} &= \Sigma_m^+ M_{m-1}^- \cdots \Sigma_{n+2}^+ M_{n+1}^- \mathcal{R}_{nn} \quad \text{if} \quad m > n,\\ \mathcal{R}_{mn} &= \Sigma_m^- M_{m+1}^+ \cdots \Sigma_{n-2}^- M_{n-1}^+ \mathcal{R}_{nn} \quad \text{if} \quad m < n.\end{aligned} \tag{22}$$

This description of the resolvent admits a simple diagrammatic representation. For example, by expanding the forward self-energy term Σ^+ into a series we see that this term regroups all paths that start from a point m and only return to it after having visited all sites $m' > m$, up to the boundary site N:

$$\begin{aligned}\Sigma_m^+ &= \frac{\mathcal{R}_m^0}{1 - \mathcal{R}_m^0 M_{m+1}^+ \Sigma_{m+2}^+ M_{m+1}^-}\\ &= \mathcal{R}_m^0 + \mathcal{R}_m^0 M_{m+1}^+ \Sigma_{m+2}^+ M_{m+1}^- \mathcal{R}_m^0 + \cdots\\ &= \mathcal{R}_m^0 + \mathcal{R}_m^0 M_{m+1}^+ \mathcal{R}_{m+2}^0 M_{m+1}^- R_m^0 + \cdots.\end{aligned} \tag{23}$$

The expansion of the forward self-energy in terms of diagrams is illustrated in Fig. 2. On the other hand, the backward self-energy term Σ^- resums loops which pass through sites $m' < m$. Equation (22) then describes the shortest path connecting a site n to site m. The role of the self-energy terms $\Sigma^{\pm}$ is to renormalize the unperturbed diagonal elements of the resolvent $\mathcal{R}_m^0 = 1/M_m^0$ by introducing a finite imaginary part, corresponding to virtual excursions to the superconducting reservoirs.

This expansion is a locator-type expansion of the resolvent, commonly used in disordered systems [59,60], in the sense that the unperturbed part of the resolvent $\mathcal{R}_m^0$ locates a quasiparticle on site m, in contrast to the more usual "propagator" which describes the propagation of a free particle. The resolvent $\mathcal{R}_{mn}$ then represents the probability that a quasiparticle is localized on site m, given that it was originally on site n. The major difference between a propagator and a locator expansion is the restriction on repeated indices which is necessary in the latter.

D. Current

Given that the dressed quasiparticle operators $\Gamma^\dagger$, Γ form a complete basis, we can express all other operators in this basis. The advantage of such decompositions is that one can then very easily derive expressions for expectation values in the stationary state $|S\rangle$, which is simply defined as the state which is annihilated by the application of the Γ operator: $\Gamma_{lk\sigma}|S\rangle = 0$.

In general, the current from a dot i to a reservoir j is given by

$$I_{i\to j}(t) = ie^{is_j\omega_0 t} d_{i\sigma}^\dagger(t)\psi_{ji\sigma}(t) - ie^{-is_j\omega_0 t}\psi_{ji\sigma}^\dagger(t) d_{i\sigma}(t), \tag{24}$$

where the shorthand $\psi_{ji\sigma}^\dagger = \sum_k J_j^\star(x_i) c_{jk\sigma}^\dagger$ is used. Creation and annihilation operators on the dots and on the leads can be expressed as functions of the dressed Floquet operators Γ:

$$\begin{aligned}d_{i\sigma}(t) &= \sum_{l,k,m}\left(e^{-i(E_{lk}+m\omega_0)t} u_m(i;lk)\Gamma_{lk\sigma} - \sigma e^{i(E_{lk}+m\omega_0)t} v_m^\star(i;lk)\Gamma_{lk-\sigma}^\dagger\right),\\ \psi_{ji\sigma}^\dagger(t) &= \sum_{l,k,m}\Big[J_j^\star(x_i)e^{i(E_{lk}+m\omega_0)t}\left(\delta_{m0}\delta_{jl}x_{jk}e^{-i\phi_j/2} + U_m^\star(j;lk)\right)\Gamma_{lk\sigma}^\dagger\\ &\quad - \sigma J_j(x_i)e^{-i(E_{lk}+m\omega_0)t}\left(\delta_{m0}\delta_{jl}y_{jk}e^{-i\phi_j/2} + V_m(j;lk)\right)\Gamma_{lk-\sigma}\Big].\end{aligned} \tag{25}$$

Since the steady state is the state which is annihilated by the operator Γ, any average taken in the steady state will contain only contributions from $\langle S|\Gamma\Gamma^\dagger|S\rangle$ terms. We then find that the steady-state current from dot i to reservoir j is

$$\langle I_{i\to j}(t)\rangle = 4\mathrm{Im}\sum_{l,k}\sum_{m,n}\left[J_j(x_i)e^{-i(m-n)\omega_0 t}(\delta_{m,s_j}\delta_{jl}y_{jk}e^{-i\phi_j/2} + V_{m-s_j}(j;lk))v_n^\star(i;lk)\right]. \tag{26}$$

Using the FLS equations (10), we can reexpress the terms involved on the right-hand side so that the current contains only quadratic terms in the resolvent. First, we reexpress the source term,

$$J_j(x_i)\delta_{m,s_j}y_{jk}e^{-i\phi_j/2} = -(E_{jk}+m\omega_0)v_m(i;jk) + \sum_{l,i'}\left[g^{21}_{l,ii'}(m-s_l)u_{m-2s_l}(i';jk) + g^{22}_{l,ii'}(m-s_l)v_m(i';jk)\right], \tag{27}$$

and the amplitudes in the reservoirs,

$$V_j(m-s_j) = \sum_{i'}\left[g^{21}_{j,ii'}(m-s_j)u_{m-2s_j}(i';l) - g^{22}_{j,ii'}(m-s_j)v_m(i';l)\right]. \tag{28}$$

The expressions we find include terms which are local, $g_{l,ii}$, and nonlocal, $g_{l,ii'}$, in the Green's functions, as well as in the resolvent (the nonlocal terms in the resolvent are its nondiagonal blocks). Note that only $g_{c,i\neq i'} \neq 0$ since only the middle superconductor S_c connects the two dots. We can therefore categorize contributions in these expressions by the number of nonlocal quantities they contain. A first approximation is to keep the "zero-order" terms, containing only local contributions. Then, the current from the dot labeled 1 to the middle superconductor is given by

$$\begin{aligned}\langle I_{1\to c}\rangle^0_{\rm dc} = 4{\rm Im}\int_\Delta^{+\infty} d\omega \sum_m \Bigg[&\begin{pmatrix} g^{21}_c(m), & -g^{22}_c(m)\end{pmatrix}\begin{pmatrix}\mathcal{R}^{11}_{m,1} & \mathcal{R}^{12}_{m,-1}\\ \mathcal{R}^{21}_{m,1} & \mathcal{R}^{22}_{m,-1}\end{pmatrix} Q_a \begin{pmatrix}\mathcal{R}^{21}_{m,1}\\ \mathcal{R}^{22}_{m,-1}\end{pmatrix}^\star \\ &-\begin{pmatrix} g^{21}_a(m+1), & -g^{22}_a(m+1)\end{pmatrix}\begin{pmatrix}\mathcal{R}^{11}_{m+2,0} & \mathcal{R}^{12}_{m+2,0}\\ \mathcal{R}^{21}_{m,0} & \mathcal{R}^{22}_{m,0}\end{pmatrix} Q_c \begin{pmatrix}\mathcal{R}^{21}_{m,0}\\ \mathcal{R}^{22}_{m,0}\end{pmatrix}^\star\Bigg].\end{aligned} \tag{29}$$

Note that this is exactly the result one would find in the case of a single junction. The resolvent elements, however, are calculated by resuming the contribution of different paths, as explained in the preceding section, and therefore take into account the effects due to the proximity of a second dot. The matrices $Q_l(\omega)$ describe the populations in the reservoirs of ejection. For the current we will take integrals over excitation energies above the gap so that $\omega > \Delta$. Then, we find that

$$Q_l(\omega) = \frac{2\Gamma_l}{\sqrt{\omega^2-\Delta^2}}\begin{pmatrix}\omega & -\Delta\\ -\Delta^* & \omega\end{pmatrix}, \quad \omega > \Delta. \tag{30}$$

If we consider that the quasiparticle density of states is [53] $\rho_S(\omega) = 2\rho_0\frac{|\omega|}{\sqrt{\omega^2-\Delta^2}}\theta(|\omega|-\Delta)$, where ρ_0 is the density of states in the normal state, we see directly that the diagonal of Q is nothing other than $\pi J^2\rho_S(\omega)$. This translates the fact that the MAR current will naturally depend on the populations of the reservoirs.

Equation (29) is at first sight not easy to calculate since it involves an integral over all quasiparticle excitation energies above the gap up to infinity, as well a summation over the Floquet harmonics. Fortunately, the resolvent elements decay exponentially at large energies, so that the integration can be drastically truncated. Moreover, at large enough voltages we observe a localization (analogous to the Wannier-Stark localization) which gives a rapidly convergent summation over the Floquet harmonics. These points will be further discussed in Sec. IV. Figures showing the localization of the resolvent elements can be found in the Supplemental Material [44].

III. SPECTROSCOPY: REVEALING THE FLOQUET-ANDREEV LADDERS

The diagonal part of the resolvent in Floquet space gives access to a spectral function. Indeed, in the case of Floquet-Green functions, one can still define a spectral function which can be interpreted as a density of states [61]. The quantity

$$\mathcal{A}(\omega) = -\frac{1}{\pi}{\rm Im}\mathcal{R}_{00}(\omega) \tag{31}$$

can be seen as a time average of the spectral function over one period of the drive. Whether we need to take the trace over the Nambu subspace of one dot or not should depend on the type of spectroscopy experiment one performs. For example, if we perform a local tunneling spectroscopy measurement on one dot, we can probe both the creation and destruction of excitations, while in an angle-resolved photoemission spectroscopy experiment we can only extract electrons, so we will only have access to one part of the spectrum [62]. In the case of local tunneling spectroscopy with a normal probe coupled to the first dot, for example, the spectral function will be given by a trace over the subspace of the first dot, defined as follows:

$$\begin{aligned}\mathcal{A}_{\rm dot1}(\omega) &= -\frac{1}{\pi}{\rm Im}{\rm Tr}_{\rm dot1}\mathcal{R}_{00}(\omega)\\ &= -\frac{1}{\pi}{\rm Im}\left[\mathcal{R}^{11}_{00}(\omega) + \mathcal{R}^{22}_{00}(-\omega)\right].\end{aligned} \tag{32}$$

The resolvent is calculated using the iterative formula of Eq. (20). In practice, we found that a cutoff index of the order of $N \sim \frac{\Delta}{\omega_0}$ is sufficient for convergence when calculating the spectral plots. Since the system we are studying is periodic in time with a period $T = \frac{2\pi}{\omega_0}$, we can plot quantities as functions of inverse voltage $\frac{1}{\omega_0}$ in order to make apparent the periodicity.

a. Floquet spectrum. Figure 3 presents the spectral function as defined in Eq. (32), calculated at a fixed distance between the two dots. At large distances compared to the superconducting length $R > \xi_0$, the energies on the first dot tend to that of a single junction, and we obtain results which agree with previous calculations done using the method of Keldysh Green's functions [37,38]. The spectrum of the single resonant dot consists of ladders of resonances at quasienergies $E_m = \epsilon_+ + 2m\omega_0$ with $\epsilon_+ = -\epsilon_-$ [38], and has a basic period of $2eV$. The Floquet ladders show avoided crossings which is

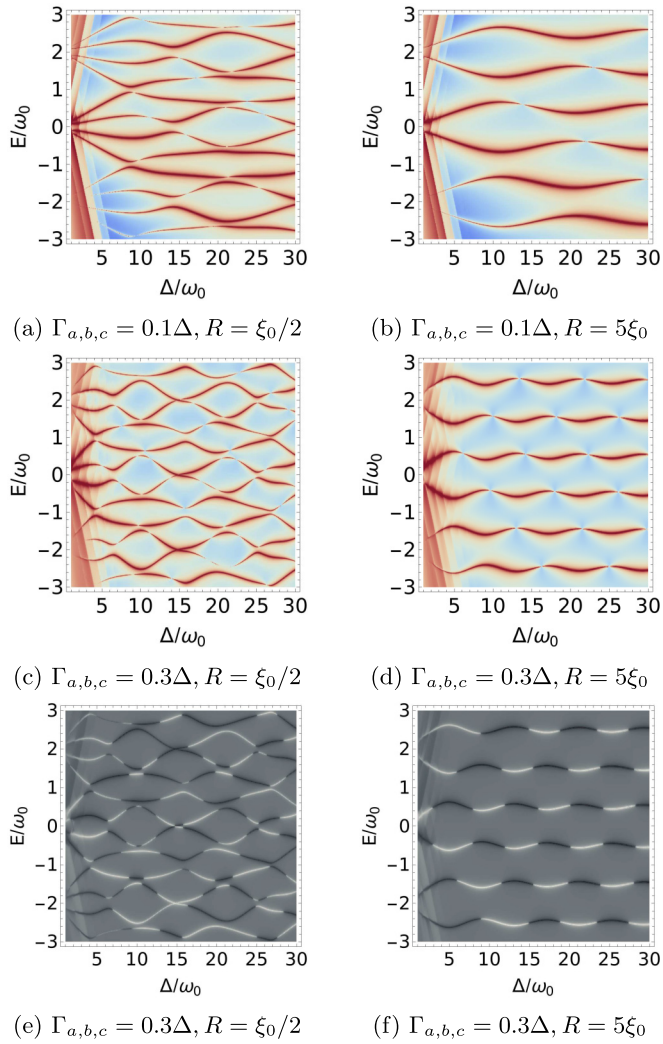

(a) $\Gamma_{a,b,c} = 0.1\Delta, R = \xi_0/2$ (b) $\Gamma_{a,b,c} = 0.1\Delta, R = 5\xi_0$

(c) $\Gamma_{a,b,c} = 0.3\Delta, R = \xi_0/2$ (d) $\Gamma_{a,b,c} = 0.3\Delta, R = 5\xi_0$

(e) $\Gamma_{a,b,c} = 0.3\Delta, R = \xi_0/2$ (f) $\Gamma_{a,b,c} = 0.3\Delta, R = 5\xi_0$

FIG. 3. [(a)–(d)] Density plots of the spectral function on the first dot, $-\frac{1}{\pi}\mathrm{Im}\mathrm{Tr}_{\mathrm{dot1}}\mathcal{R}_{00}$, plotted using inverse scaling. Red corresponds to the maxima of the spectral function. The distance between the dots is taken to be [(a), (c), (e)] $R = \xi_0/2$ and [(b), (d), (f)] $R = 5\xi_0$. [(e), (f)] Particle-hole asymmetry of the spectral function $-\frac{1}{\pi}\mathrm{Im}[\mathcal{R}^{11}_{00}(\omega) - \mathcal{R}^{22}_{00}(\omega)]$. White represents positive values of the difference (electronlike) and black represents negative values (holelike). The signs change at avoided crossings.

a sign of coupling between them via Landau-Zener transitions. Both electronic and hole parts of the resolvent have peaks at the same energies, but their weight away from avoided crossings differs when varying the voltage. To illustrate this, we plot the difference between the electron and hole parts of the spectral function $-\frac{1}{\pi}\mathrm{Im}[\mathcal{R}^{11}_{00}(\omega) - \mathcal{R}^{22}_{00}(\omega)]$ in Figs. 3(e) and 3(f). Near avoided crossings, a rapid change of the Floquet states is expected to happen. Accordingly, we see that the sign of the aforementioned quantity changes signs at avoided crossings, signaling the change in character between electronlike and holelike states. In order to observe this asymmetry it would be necessary to break the mirror symmetry of the system, for example by having asymmetric tunnel couplings. One could then probe the asymmetry away from avoided crossings by measuring the conductance at opposite voltage values, as has been proposed in Ref. [63].

b. Floquet engineering. The avoided crossings present in Fig. 3 could be used to find dynamical sweet spots of the system. These so-called sweet spots are optimal working points corresponding to the extrema in quasienergy differences and have been proposed as a way to protect qubits from noise. Contrary to the static case where few sweet spots are present, the extra dimension of time in periodically driven systems allows to find a manifold of dynamical sweet spots [26]. An added advantage is that one can tune the system to an avoided crossing by changing the drive *in situ*. Realization of a Floquet qubit has been proposed along this line [28], where a periodic driving can be used to tune the system near one of the avoided crossings, and a second drive can be used to control transitions between the Floquet states. Typically, the smaller the quasienergy dispersion, the more insensitive would the qubit states be to fluctuations. Moreover, tuning a fluxonium qubit to a dynamical sweet spot away from its half-flux bias static spot has been shown to increase coherence times [27], demonstrating the relevance of Floquet engineering to the qubit community. Some more Floquet spectra for different combinations of tunnel couplings are presented in the Supplemental Material [44], showing various different possibilities when engineering the band structure.

c. Level splitting. When the distance between the dots is comparable to the superconducting coherence length $R \sim \xi_0$, we arrive at an "Andreev molecule regime," where a lift of degeneracy produces four peaks instead of two in each Floquet-Brillouin zone. At large distances the splitting decreases exponentially with the distance $\sim e^{-R/\xi_0}$. However, at intermediate distances its behavior depends on the applied voltage. Figure 4 shows the lift of degeneracy of the quasienergy levels when the two dots are brought close together. In reality, we observe *oscillations* of the spectral functions around the single-junction value even at very large distances. We discuss this long-range interference effect in Sec. IV B and show that the oscillations of the spectral functions lead to an oscillatory I-V curve.

IV. SUBGAP CURRENT

Before showing the results for the Andreev molecule, we will briefly discuss the well-known case of a single junction. This serves two purposes, the first being to benchmark our method by comparing with what is already known, and the second to acquaint the reader with the Floquet ladder and its impact on the current.

A. Current through one resonant dot from the point of view of its Floquet spectrum

The symmetric configuration of a resonant dot with energy $\epsilon_d = 0$ coupled to two reservoirs which are voltage biased with $(V_L = -V, V_R = +V)$ is already well understood: the subgap structure of the current-voltage curve shows steps at voltages $2eV = \frac{2\Delta}{n}$, and the presence of the resonant level restricts n to being an odd integer, while even MAR processes are suppressed [33–36]. These steps in the subgap current appear whenever a new "MAR trajectory" becomes

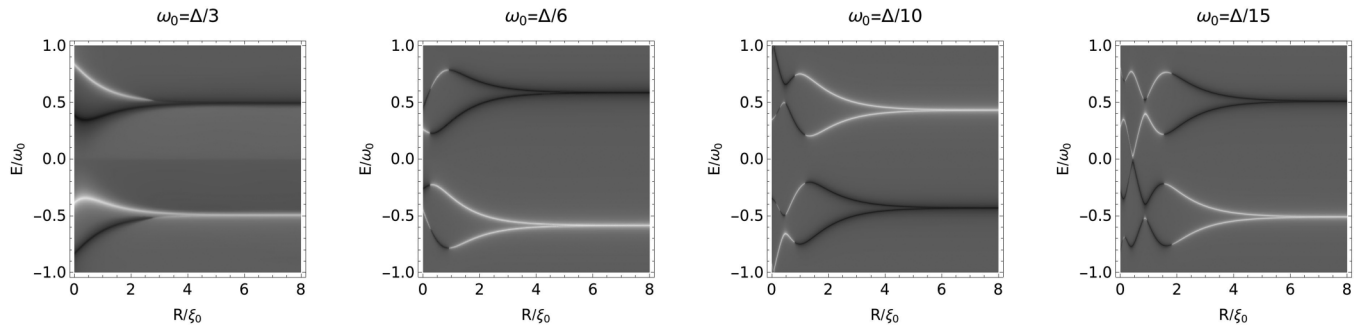

FIG. 4. Density plots of $-\frac{1}{\pi}\mathrm{Im}[\mathcal{R}^{11}_{00}(\omega)-\mathcal{R}^{22}_{00}(\omega)]$ as a function of the distance between the two dots, for different values of voltage bias ω_0. At large distances $R \gg \xi_0$ the quasienergies approach those of a single junction. At $R \sim \xi_0$ we are in a molecular regime, and there is a considerable lift of degeneracy of the quasienergies. White represents positive values of the difference (electronlike) and black represents negative values (holelike). We set $k_F R = \pi/4$ and $\Gamma_{a,b,c} = 0.3\Delta$.

possible: a quasiparticle is Andreev reflected n times, changing its energy by $e(V_R - V_L) = 2eV$ with each reflection, until it has enough energy (equivalent to the size of the gap 2Δ) to reach the superconducting continuum of states and give a contribution to the current. The results of our calculation for this case are depicted in Fig. 5(a) for different values of tunnel couplings $\Gamma = \Gamma_L = \Gamma_R$, and we verify that our method gives the expected results for the I-V curves at zero temperature. In order to produce this result, we numerically calculated the current given by the following formula:

$$\langle I_{\mathrm{dot}\to R}\rangle_{\mathrm{dc}} = 4\mathrm{Im}\int_{\Delta}^{+\infty} d\omega \sum_m \Big[\big(g_L^{21}(m+1),\, g_L^{22}(m+1)\big) \times \begin{pmatrix} \mathcal{R}^{11}_{m+2,-1} & \mathcal{R}^{12}_{m+2,1} \\ \mathcal{R}^{21}_{m,-1} & \mathcal{R}^{22}_{m,1} \end{pmatrix} Q_R \begin{pmatrix} \mathcal{R}^{21}_{m,-1} & \mathcal{R}^{22}_{m,1} \end{pmatrix}^{\star} - \big(g_R^{21}(m-1),\quad g_R^{22}(m-1)\big) \times \begin{pmatrix} \mathcal{R}^{11}_{m-2,1} & \mathcal{R}^{12}_{m-2,-1} \\ \mathcal{R}^{21}_{m,1} & \mathcal{R}^{22}_{m,-1} \end{pmatrix} Q_L \begin{pmatrix} \mathcal{R}^{21}_{m,1} & \mathcal{R}^{22}_{m,-1} \end{pmatrix}^{\star} \Big]. \tag{33}$$

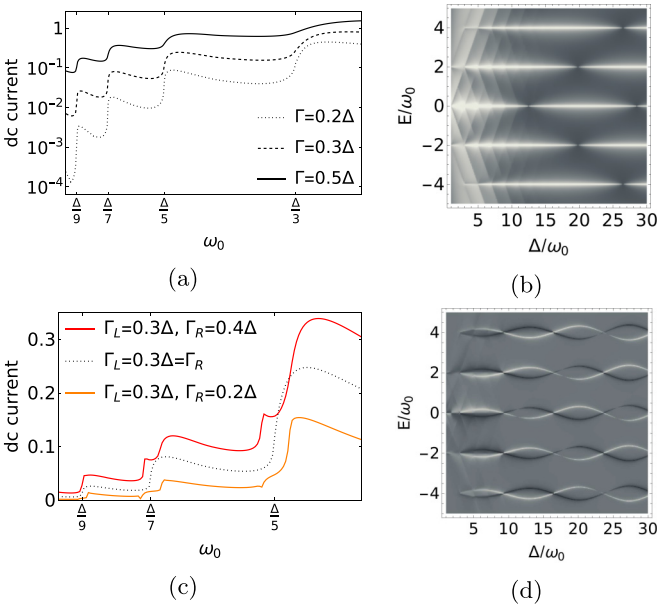

FIG. 5. Subgap current and corresponding Floquet spectra of a single resonant dot. (a) Subgap structure for the highly symmetric left-right configuration $\Gamma = \Gamma_L = \Gamma_R$ and $(V_L = -V, V_R = +V)$ with the known MAR steps at odd subdivisions of the gap. Logarithmic scaling has been used for better visibility of the features. (b) The corresponding Floquet spectrum consists of decoupled ladders at multiples of the basic frequency $2\omega_0$. The maxima of the spectral function are shown here in white. (c) Comparison of subgap current for equal (dashed black line) and unequal (red and orange lines) tunnel couplings ($\Gamma_L \neq \Gamma_R$), showing the modification of the MAR steps when there is asymmetry in the tunnel couplings. (d) Particle-hole asymmetry $-\mathrm{Im}[\mathcal{R}^{11}_{00}(\omega) - \mathcal{R}^{22}_{00}(\omega)]$ for $\Gamma_L = 0.3\Delta$, $\Gamma_R = 0.4\Delta$.

We see that the current requires calculation of the resolvent elements $\mathcal{R}_{m,n}$ which connect the "source sites" at $n = V_{L,R}/V = \pm 1$ on the Floquet chain to sites on positions m. These nondiagonal elements correspond to processes where the system changes its energy by $|m-n|\omega_0$, equivalent to absorbing or emitting an $|m-n|$ number of "photons."

a. Resolvent resonant structure. In the previous section we have seen that the resolvent $\mathcal{R}_{00}$ has resonances at even multiples of ω_0: outside the gap the spectrum shows signs of dissipation because of strong hybridization with the reservoirs, i.e., the resolvent decays exponentially for large energies $\omega \gg \Delta$. Floquet resonances, however, "survive" around frequencies $\omega_0 > \Delta/n$, with n the smallest even number such that the condition holds. The peaks are sharper at small voltages, and become smeared when increasing ω_0. The symmetry by translation of the resolvent $\mathcal{R}_{m,n}(\omega + p\omega_0) = \mathcal{R}_{m+p,n+p}(\omega)$ means that elements $\mathcal{R}_{\pm1,\pm1}(\omega) = \mathcal{R}_{00}(\omega \pm \omega_0)$ have resonance peaks around odd multiples of ω_0, which gives the condition for the MAR steps at odd subdivisions of the gap in the presence of a resonant level. Moreover, since the nondiagonal elements of the resolvent $\mathcal{R}_{m,\pm1}$ are obtained from the diagonal elements $\mathcal{R}_{\pm1,\pm1}$ through Eq. (22) we can conclude two things: (a) they are resonant when the corresponding diagonal elements are resonant, and (b) there is a hierarchy of peaks in m which depends on the voltage. An element $\mathcal{R}_{m,\pm1}$ becomes dominant when $m\omega_0$ is the dominant peak above the gap, i.e., when m is the minimal odd integer for which $m\omega_0 > \Delta$. For example, the element $R_{-3,-1}$ is dominant when the second-order MAR trajectory is dominant, $\frac{\Delta}{3} < \omega_0 < \Delta$, the element $R_{-5,-1}$ is dominant when the

third-order MAR trajectory is dominant, $\frac{\Delta}{5} < \omega_0 < \frac{\Delta}{3}$, and so on. The resonant structure of the resolvent is illustrated with some more detail in the Supplemental Material [44].

The localization on the Floquet chain can be further illustrated by decomposing the subgap current into the contribution from each Floquet harmonic. Then, we find that at large voltages only a few harmonics need to be taken into account when calculating the sum in Eq. (33), and the number of harmonics needed increases as the voltage goes to zero. We will show, and further discuss, this localization in the case of the Andreev molecule (Fig. 8), but a completely analogous result holds for the single junction case.

b. Asymmetry effects. It has perhaps been less commented in the literature that the subgap current steps appear at exactly $\omega_0 = \frac{\Delta}{n}$ only when there is a "left-right" parity symmetry which happens when the tunnel couplings to the reservoirs are equal, $\Gamma_L = \Gamma_R$, and the voltage biasing is symmetric around the dot energy, $V_L = -V_R$. In this mirror-symmetric case, electronlike and holelike MAR trajectories are equally favorable. The corresponding spectrum then consists of degenerate ladders situated exactly at even multiples of ω_0. The Floquet ladders are completely decoupled and show no avoided-crossing behavior, as shown in Fig. 5(b). When this symmetry is broken, we find that the electronlike part $-\mathrm{Im}\mathcal{R}^{11}_{00}(\omega)$ and the holelike part $-\mathrm{Im}\mathcal{R}^{22}_{00}(\omega)$ of the spectrum have peaks at different energies $E_m = m\omega_0 \pm \epsilon$, as has been already noted [37,38]. We find that the current carries a trace of this characteristic of the spectrum: the MAR steps break into two substeps, positioned around the original $\omega_0 = \frac{\Delta \pm \epsilon}{n}$ frequencies. The exact shape of the steps (cusps or peaks) depends on the choice of the couplings [64], as shown in Fig. 5(c). This result suggests that electron-boson interaction (such as absorption or emission of photons by the tunneling quasiparticles), as studied in Ref. [65], is not sufficient to break particle-hole symmetry of the conductance, but also requires a breaking of the mirror symmetry of the system. In Ref. [65] the mirror symmetry was broken by considering an N-S system.

B. Current through the driven Andreev molecule

a. Modification of the subgap structure. The main result for the bijunction current is presented in Fig. 6, where we plot the results of numerical calculations of Eq. (29). For simplicity, we consider equal tunnel couplings $\Gamma_a = \Gamma_b = \Gamma_c = 0.3\Delta$, and we fix $k_F R = \pi/4$, in order to avoid oscillations on the scale of the Fermi wavelength. We see that for large distances between the dots (grey line) the I-V curve approaches that of a single S-dot-S junction (dashed black line). In reality, at large distances, the curves show oscillations around the single junction curve; this will be commented on shortly. For distances comparable to the superconducting length (red and orange lines), we are clearly in a "molecular junction" regime [66], and the MAR steps break into four substeps. These substeps correspond to the splitting of the energy levels in the Floquet spectrum in the Andreev molecule regime, as discussed earlier (see Fig. 3). The steps are visible when the resonances are not overlapping, that is, when their widths are smaller than their separation. Given that the width of a resonance coupled to a continuum of states increases when the coupling to the continuum is increased, one expects that small values of voltage bias and tunnel couplings give sharper features. Indeed, the new features due to the proximity of a second junction are more clear at voltages equal to higher-order subdivisions of the gap. However, the modification should still be visible around the $\frac{2\Delta}{3}$ or the $\frac{2\Delta}{5}$ MAR steps. Moreover, the influence of the tunnel couplings on the I-V curves is shown in Fig. 7. As it is expected we observe that the subgap features are softened when increasing the tunnel coupling to the reservoirs.

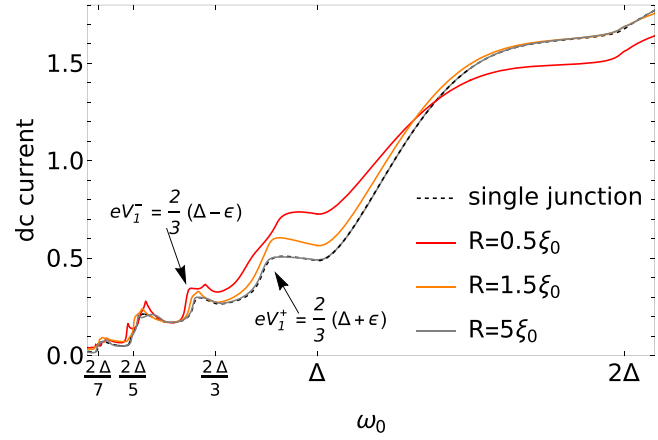

FIG. 6. Andreev molecule I-V curve calculated at various distances between the two dots. Parameters used: $\Gamma_{a,b,c} = 0.3\Delta$, $k_F R = \pi/4$, $\phi_{a,b,c} = 0$.

b. Contribution of Floquet harmonics. Depending on the region of the I-V curve the sum over the Floquet modes in Eq. (29) of the current can be drastically truncated, and the larger the voltage drive, the less harmonics we need to sum over. We therefore have a "localization" on the Floquet chain, analogous to the Wannier-Stark localization of electrons in solids at strong electric fields. This localization is illustrated in Fig. 8. At large voltages $\omega_0 > 2\Delta$, the drive is strong enough to promote quasiparticles directly above the gap without any MAR processes, and we only need to sum over two harmonics $m = \pm 1$. As we lower the voltage, we progressively need

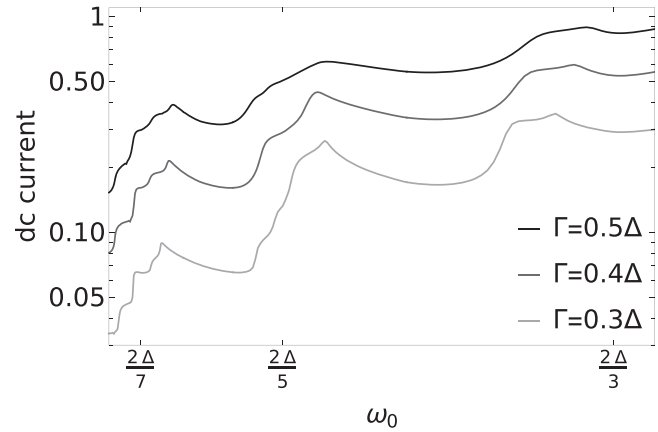

FIG. 7. Andreev molecule I-V curves for different values of tunnel coupling $\Gamma_{a,b,c} = \Gamma$, at fixed distance between the dots $R = \xi_0$. Logarithmic scaling is used. Features are softened with increasing Γ and voltage.

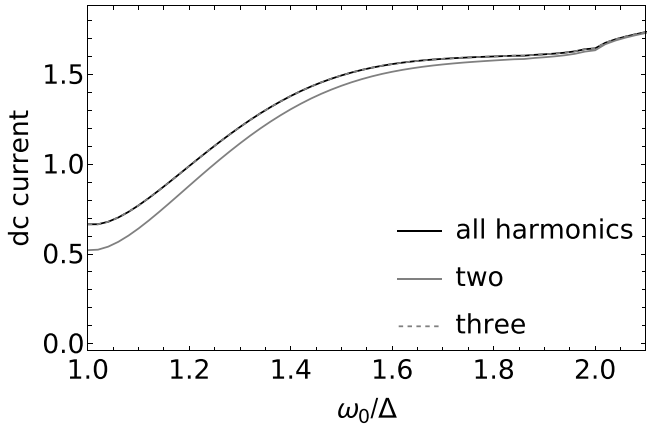

(a)

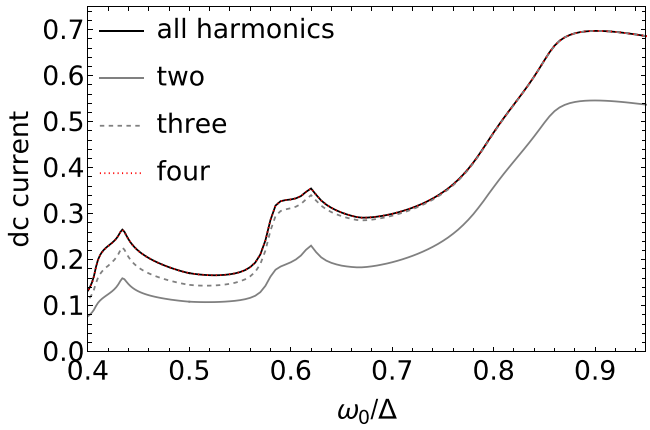

(b)

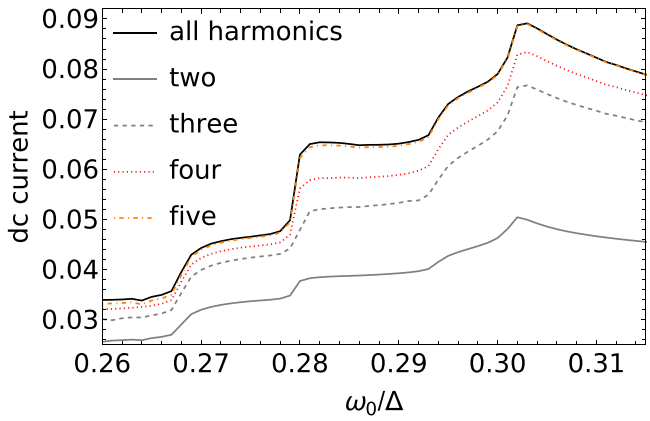

(c)

FIG. 8. "Localization" on the Floquet chain means only a few of the harmonics need to be taken into account when calculating the current. The amount of harmonics required increases with decreasing voltage. Parameters: $R = \xi_0$, $\Gamma_{a,b,c} = 0.3\Delta$, $k_F R = \pi/4$.

to add more harmonics, in correspondence to the MAR processes which are dominant. In the region of the first allowed MAR process, $\frac{2\Delta}{3} < \omega_0 < 2\Delta$, the current is well approximated by summing over three harmonics $m = \pm 1, -3$; in the next region of $\frac{2\Delta}{5} < \omega_0 < \frac{2\Delta}{3}$, we need to add one more $m = \pm 1, -3, -5$, and so on.

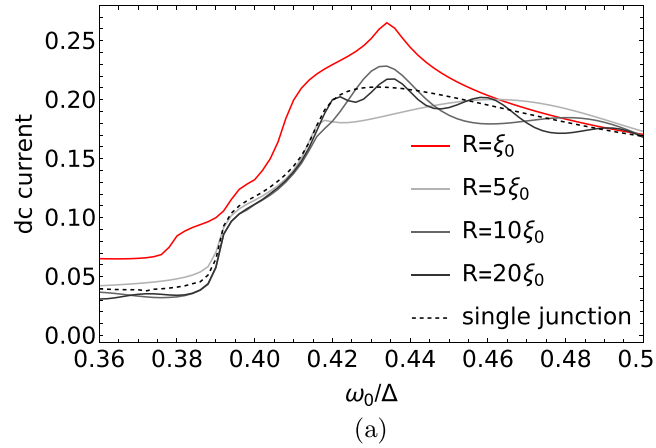

(a)

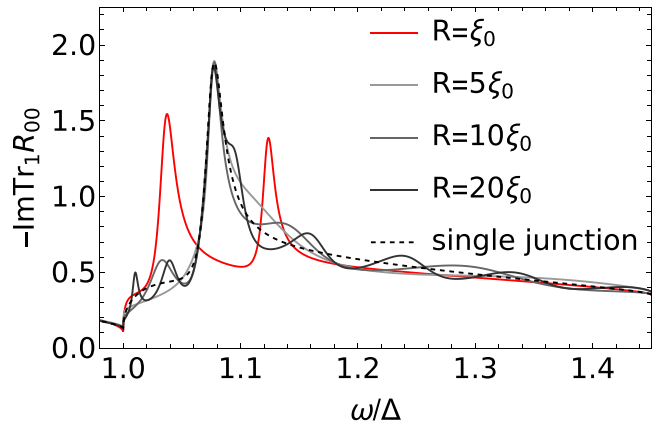

(b)

FIG. 9. Long-range Floquet-Tomasch effect. (a) Subgap current structure near the second MAR step, around $\omega_0 = \frac{2\Delta}{5}$, compared to the single junction case (in red). At large distances (gray lines) oscillations of the I-V curves appear around the single junction current. (b) Spectral function at energies above the superconducting gap, for $\omega_0 = 0.45\Delta$.

C. Long-range Floquet-Tomasch oscillations

The effect of the distance between the dots is shown with more detail in Fig. 9, focusing on the region of the MAR step around $\omega_0 = \frac{2\Delta}{5}$. We observe that an increased distance (grey lines) produces oscillations of the I-V curve itself around the single junction curve (dashed line). Moreover, the splitting between the Floquet-Andreev resonances is suppressed exponentially with the distance (see Fig. 4), so that at large distances we can only see the steps corresponding to the poles of the single junction resolvent. The effect at large distances is reminiscent of the Tomasch effect. Historically, Tomasch [41] observed oscillations in the density of states above the gap and in the tunneling current. The oscillations depend on the applied voltage and the thickness d of superconducting films as a function of the combination $\frac{2d\sqrt{(eV)^2-\Delta^2}}{\hbar v_F}$. Following the experimental observation, McMillan and Anderson [42] then interpreted the phenomenon as one of quasiparticle interference due to a perturbation in the order parameter (induced by some impurity or by some spatially nonuniform Δ). Figure 9(b) shows the spectral function $-\mathrm{Im}\mathrm{Tr}_{\mathrm{dot1}}\mathcal{R}_{00}$ at energies above the gap, calculated at a fixed voltage value

$\omega_0 = 0.45\Delta$. We observe that at large distances the spectral function oscillates around the spectral function of the single junction. We find that the frequency of oscillations *is* the Tomasch frequency, and we provide a demonstration in the Appendix to support this observation. It has been argued [43] that this new "Floquet-Tomasch" effect could be used to create correlations of Cooper pairs over long distances, which are orders of magnitude larger than the superconducting coherence length (in the Tomasch experiment the thickness was some tens of micrometers, 10–30 μm $\sim 100\xi_0$). It is a nonlocal effect over distances which are not achievable in the absence of the voltage drive since it is mediated by quasiparticles which, by MAR processes, reach the continuum of states of the middle superconductor S_c where they can propagate over a long distance without being bound by the superconducting coherence length.

V. SUMMARY AND PERSPECTIVES

In conclusion, we have studied the Andreev molecule subjected to a dc voltage drive, which brings the system out of equilibrium. The superconductivity of the leads allows to explore Floquet physics by simple voltage biasing. As is often done in Floquet systems [21], one can expand quantities, such as the electron and hole amplitudes on the dot(s), into Fourier modes and map the initial time-dependent BdG equation into a tight-binding chain with sites labeled by the Fourier harmonics. The sites are coupled to their nearest neighbors through absorption or emission of virtual photons which here correspond to Andreev reflections. The tight-binding analogy can be exploited to get an iterative solution that corresponds to a Dyson equation for the Green's function on the dot(s). We find that the initial discrete levels are renormalized by a self-energy which corresponds to the sum of two independent processes, the $\Sigma^{\pm}$ of Eq. (21). These matrices describe loops that connect the initial discrete levels to the superconducting continua either above the gap, $\omega > \Delta$, or below the gap, $\omega < -\Delta$, and therefore are a source of dissipation. An effective Hamiltonian for the amplitudes on the dot(s) will therefore be non-Hermitian, since the S-dot-S system in the presence of voltage is an open quantum system.

The resonances on the dots are then coupled through the middle reservoir by the nonlocal Green's function of Eq. (12). This coupling produces splitting of the energy levels and avoided crossings in the spectrum at distances between the dots comparable to the superconducting coherence length $R \sim \xi_0$. It also modifies the subgap structure, producing splitting of the MAR steps. This direct coupling decays exponentially with R/ξ_0. Instead, at $R \gg \xi_0$ the two dots are coupled through higher-order processes contained in the self-energy which become the dominant mechanism for coupling at long distances. This long-range Floquet-Tomasch mechanism involves local MAR processes on each dot and subsequent quasiparticle propagation through the middle superconductor at energies $|\omega| > \Delta$. The system in this regime behaves like an interferometer, in the sense that the current becomes an oscillatory function of the voltage. We intend to further explore this in upcoming work, particularly in relation to the spectral properties of the system, since the Floquet-Tomasch effect is expected to cause interference effects on the subgap resonances as well.

This study could allow interpreting the signatures of an Andreev molecule in nonequilibrium dc transport experiments, an understanding that was missing so far. Moreover, the method we have employed can be adapted to accommodate various different and more complex situations, such as multilevel dots, or multiterminal configurations. Open questions remain as to the effect of the interactions, which could be added perturbatively at the limit $U/\Gamma < 1$ in the spirit of Ref. [67]. However, subsequent work shows that this approach seems to fail at the MAR points [68], so a better method might be needed.

ACKNOWLEDGMENTS

We wish to thank Ç. Girit for some very helpful discussions. B.D. also thanks Régis Mélin for sharing his results on long-range Floquet-Tomasch correlations before their publication [43], and for many stimulating discussions.

APPENDIX: OSCILLATIONS ABOVE THE GAP

For energies above the gap $\omega > \Delta$, we have seen that the spectral function on dot 1, given by

$$\mathcal{A}(\omega) = -2\mathrm{Im}\mathcal{R}_{00}^{11}(\omega) = -\mathrm{Im}\big[\mathcal{R}_{00}^{11}(\omega) + \mathcal{R}_{00}^{22}(-\omega)\big],$$

oscillates as a function of the energy ω and the distance R separating dot 1 and dot 2, a phenomenon reminiscent of the Tomasch oscillations. In fact, we will show that the oscillations of the spectral function are due to a "Tomasch phase factor" equal to $e^{2i\sqrt{\omega^2-\Delta^2}R/v_F}$, and will explain the physical process that, in this case, gives rise to the oscillations.

In order to calculate the resolvent above the gap, we can neglect the forward self-energies Σ^{+}, given in Eq. (21). The resolvent can then be written as

$$\mathcal{R}_{00} = [M^0(0) - \Sigma^-(0)]^{-1}, \tag{A1}$$

with the backward self-energy given by

$$\begin{aligned}\Sigma^-(0) &\equiv \begin{pmatrix} \Sigma_1^-(0) & \Sigma_{12}^-(0) \\ \Sigma_{21}^-(0) & \Sigma_2^-(0) \end{pmatrix} \\ &= M^-(-1)\frac{1}{M^0(-2) - \Sigma^-(-2)}M^+(-1).\end{aligned} \tag{A2}$$

We would like to compare the spectral function of the bijunction system on dot 1 to that of a single junction. We must therefore define the latter: if the distance between the dots $R \to \infty$, then the resolvent of dot 1 (dot 2) would be

$$\mathcal{R}_{1(2)} = \big[M_{1(2)}^0(0) - \Sigma_{1(2)}^-(0)\big]^{-1}, \tag{A3}$$

where all matrices are now calculated in the 2×2 subspace of dot 1 (dot 2). The backward self-energies $\Sigma_{1(2)}^-(0)$ represent *local* MAR processes which connect the state on dot 1 (dot 2) above the gap to those below the gap.

The resolvent (A1) of the bijunction system can the be written as a block matrix:

$$\begin{aligned}\mathcal{R}_{00} &= \begin{pmatrix} M_1^0(0) - \Sigma_1^-(0) & g_c(0,R) - \Sigma_{12}^-(0) \\ g_c(0,R) - \Sigma_{21}^-(0) & M_2^0(0) - \Sigma_2^-(0) \end{pmatrix}^{-1} \\ &\approx \begin{pmatrix} M_1^0(0) - \Sigma_1^-(0) & g_c(0,R) \\ g_c(0,R) & M_2^0(0) - \Sigma_2^-(0) \end{pmatrix}^{-1}.\end{aligned} \tag{A4}$$

We can neglect the matrices $\Sigma^{-}_{12,21}$ in the off diagonal, since they are of higher order in the tunnel couplings. The resolvent (A4) therefore describes resonances on each dot which are formed due to local MAR processes and which are then coupled by propagation in the middle reservoir, represented by the nonlocal Green's function $g_c(0, R)$ in the off diagonal.

Since the resolvent is a block matrix, we can invert it blockwise [69]. For the resolvent of Eq. (A4), the upper-left block (corresponding to the first dot) is

$$[\mathcal{R}_{00}]_{\rm dot1} = \frac{\mathcal{R}_1}{1 - \mathcal{R}_1 g_c(0,R)\mathcal{R}_2 g_c(0,R)} \approx \mathcal{R}_1 + \mathcal{R}_1 g_c(0,R)\mathcal{R}_2 g_c(0,R)\mathcal{R}_1 + \cdots . \quad \text{(A5)}$$

We therefore find that the first correction to the resolvent of the two coupled dots with respect to the resolvent corresponding to an uncoupled dot is

$$[\mathcal{R}_{00}]_{\rm dot1} - \mathcal{R}_1 \approx \mathcal{R}_1 g_c(0,R)\mathcal{R}_2 g_c(0,R)\mathcal{R}_1 . \quad \text{(A6)}$$

A term like the above has a clear physical interpretation: the two resonances represented by $\mathcal{R}_{1,2}$ are coupled via propagating quasiparticles in the continuum of states of the middle superconductor. The amplitude of the effect will therefore depend on the specific geometry of the middle reservoir (here we have considered a one-dimensional superconducting wire). We see that the Tomasch phase factor will appear, since the nonlocal Green's function $g_c(0, R)$ is proportional to a phase $e^{i\sqrt{\omega^2-\Delta^2}R/v_F}$. A phase $e^{2i\sqrt{\omega^2-\Delta^2}R/v_F}$ is then accumulated by quasiparticles which travel from resonance 1 to resonance 2 and back. Therefore, at a fixed distance R, the resolvent of the coupled system oscillates as a function of the energy around the single-dot resolvent $\mathcal{R}_1$.

[1] M. H. Devoret and R. J. Schoelkopf, Superconducting circuits for quantum information: An outlook, Science **339**, 1169 (2013).

[2] B. Josephson, Possible new effects in superconductive tunnelling, Phys. Lett. **1**, 251 (1962).

[3] P. W. Anderson and J. M. Rowell, Probable Observation of the Josephson Superconducting Tunneling Effect, Phys. Rev. Lett. **10**, 230 (1963).

[4] M. A. Despósito and A. Levy Yeyati, Controlled dephasing of Andreev states in superconducting quantum point contacts, Phys. Rev. B **64**, 140511(R) (2001).

[5] A. Zazunov, V. S. Shumeiko, E. N. Bratus', J. Lantz, and G. Wendin, Andreev Level Qubit, Phys. Rev. Lett. **90**, 087003 (2003).

[6] N. M. Chtchelkatchev and Y. V. Nazarov, Andreev Quantum Dots for Spin Manipulation, Phys. Rev. Lett. **90**, 226806 (2003).

[7] C. Janvier, L. Tosi, L. Bretheau, Ç. Ö. Girit, M. Stern, P. Bertet, P. Joyez, D. Vion, D. Esteve, M. F. Goffman, H. Pothier, and C. Urbina, Coherent manipulation of Andreev states in superconducting atomic contacts, Science **349**, 1199 (2015).

[8] R.-P. Riwar, M. Houzet, J. S. Meyer, and Y. V. Nazarov, Multi-terminal Josephson junctions as topological matter, Nat. Commun. **7**, 11167 (2016).

[9] B. Douçot, R. Danneau, K. Yang, J.-G. Caputo, and R. Mélin, Berry phase in superconducting multiterminal quantum dots, Phys. Rev. B **101**, 035411 (2020).

[10] A. Freyn, B. Douçot, D. Feinberg, and R. Mélin, Production of Nonlocal Quartets and Phase-Sensitive Entanglement in a Superconducting Beam Splitter, Phys. Rev. Lett. **106**, 257005 (2011).

[11] T. Jonckheere, J. Rech, T. Martin, B. Douçot, D. Feinberg, and R. Mélin, Multipair dc Josephson resonances in a biased all-superconducting bijunction, Phys. Rev. B **87**, 214501 (2013).

[12] A. H. Pfeffer, J. E. Duvauchelle, H. Courtois, R. Mélin, D. Feinberg, and F. Lefloch, Subgap structure in the conductance of a three-terminal Josephson junction, Phys. Rev. B **90**, 075401 (2014).

[13] Y. Cohen, Y. Ronen, J.-H. Kang, M. Heiblum, D. Feinberg, R. Mélin, and H. Shtrikman, Nonlocal supercurrent of quartets in a three-terminal Josephson junction, Proc. Natl. Acad. Sci. USA **115**, 6991 (2018).

[14] J.-D. Pillet, V. Benzoni, J. Griesmar, J.-L. Smirr, and Ç. Ö. Girit, Nonlocal Josephson effect in Andreev molecules, Nano Lett. **19**, 7138 (2019).

[15] J. D. Pillet, V. Benzoni, J. Griesmar, J. L. Smirr, and Ç. Ö. Girit, Scattering description of Andreev molecules, SciPost Phys. Core **2**, 009 (2020).

[16] O. Kürtössy, Z. Scherübl, G. Fülöp, I. E. Lukács, T. Kanne, J. Nygård, P. Makk, and S. Csonka, Andreev molecule in parallel InAs nanowires, Nano Lett. **21**, 7929 (2021).

[17] S. Matsuo, J. S. Lee, C.-Y. Chang, Y. Sato, K. Ueda, C. J. Palmstrøm, and S. Tarucha, Observation of nonlocal Josephson effect on double InAs nanowires, Commun. Phys. **5**, 221 (2022).

[18] J. D. Sau and S. D. Sarma, Realizing a robust practical Majorana chain in a quantum-dot-superconductor linear array, Nat. Commun. **3**, 964 (2012).

[19] M. Leijnse and K. Flensberg, Parity qubits and poor man's Majorana bound states in double quantum dots, Phys. Rev. B **86**, 134528 (2012).

[20] S. Kohler, J. Lehmann, and P. Hänggi, Driven quantum transport on the nanoscale, Phys. Rep. **406**, 379 (2005).

[21] T. Oka and S. Kitamura, Floquet engineering of quantum materials, Annu. Rev. Condens. Matter Phys. **10**, 387 (2019).

[22] J. Cayssol, B. Dóra, F. Simon, and R. Moessner, Floquet topological insulators, Phys. Status Solidi RRL **7**, 101 (2013).

[23] M. S. Rudner and N. H. Lindner, Band structure engineering and non-equilibrium dynamics in Floquet topological insulators, Nat. Rev. Phys. **2**, 229 (2020).

[24] L. Broers and L. Mathey, Observing light-induced Floquet band gaps in the longitudinal conductivity of graphene, Commun. Phys. **4**, 248 (2021).

[25] J. W. McIver, B. Schulte, F.-U. Stein, T. Matsuyama, G. Jotzu, G. Meier, and A. Cavalleri, Light-induced anomalous Hall effect in graphene, Nat. Phys. **16**, 38 (2020).

[26] Z. Huang, P. S. Mundada, A. Gyenis, D. I. Schuster, A. A. Houck, and J. Koch, Engineering Dynamical Sweet Spots to Protect Qubits from $1/f$ Noise, Phys. Rev. Appl. **15**, 034065 (2021).

[27] P. S. Mundada, A. Gyenis, Z. Huang, J. Koch, and A. A. Houck, Floquet-Engineered Enhancement of Coherence Times in a Driven Fluxonium Qubit, Phys. Rev. Appl. **14**, 054033 (2020).

[28] A. Gandon, C. Le Calonnec, R. Shillito, A. Petrescu, and A. Blais, Engineering, Control, and Longitudinal Readout of Floquet Qubits, Phys. Rev. Appl. **17**, 064006 (2022).

[29] A. Lazarides, A. Das, and R. Moessner, Equilibrium states of generic quantum systems subject to periodic driving, Phys. Rev. E **90**, 012110 (2014).

[30] S. Park, W. Lee, S. Jang, Y.-B. Choi, J. Park, W. Jung, K. Watanabe, T. Taniguchi, G. Y. Cho, and G.-H. Lee, Steady Floquet–Andreev states in graphene Josephson junctions, Nature (London) **603**, 421 (2022).

[31] T. Klapwijk, G. Blonder, and M. Tinkham, Explanation of subharmonic energy gap structure in superconducting contacts, Physica B+C **109-110**, 1657 (1982).

[32] E. N. Bratus', V. S. Shumeiko, and G. Wendin, Theory of Subharmonic Gap Structure in Superconducting Mesoscopic Tunnel Contacts, Phys. Rev. Lett. **74**, 2110 (1995).

[33] A. L. Yeyati, J. C. Cuevas, A. López-Dávalos, and A. Martín-Rodero, Resonant tunneling through a small quantum dot coupled to superconducting leads, Phys. Rev. B **55**, R6137 (1997).

[34] G. Johansson, E. N. Bratus, V. S. Shumeiko, and G. Wendin, Resonant multiple Andreev reflections in mesoscopic superconducting junctions, Phys. Rev. B **60**, 1382 (1999).

[35] T. Jonckheere, A. Zazunov, K. V. Bayandin, V. Shumeiko, and T. Martin, Nonequilibrium supercurrent through a quantum dot: Current harmonics and proximity effect due to a normal-metal lead, Phys. Rev. B **80**, 184510 (2009).

[36] A. Martín-Rodero and A. L. Yeyati, Josephson and Andreev transport through quantum dots, Adv. Phys. **60**, 899 (2011).

[37] R. Mélin, J.-G. Caputo, K. Yang, and B. Douçot, Simple Floquet-Wannier-Stark-Andreev viewpoint and emergence of low-energy scales in a voltage-biased three-terminal Josephson junction, Phys. Rev. B **95**, 085415 (2017).

[38] R. Mélin, R. Danneau, K. Yang, J.-G. Caputo, and B. Douçot, Engineering the Floquet spectrum of superconducting multiterminal quantum dots, Phys. Rev. B **100**, 035450 (2019).

[39] G. H. Wannier, Wave functions and effective Hamiltonian for Bloch electrons in an electric field, Phys. Rev. **117**, 432 (1960).

[40] E. E. Mendez and G. Bastard, Wannier-Stark ladders and Bloch oscillations in superlattices, Phys. Today **46**, 34 (1993).

[41] W. J. Tomasch, Geometrical Resonance in the Tunneling Characteristics of Superconducting Pb, Phys. Rev. Lett. **15**, 672 (1965).

[42] W. L. McMillan and P. W. Anderson, Theory of Geometrical Resonances in the Tunneling Characteristics of Thick Films of Superconductors, Phys. Rev. Lett. **16**, 85 (1966).

[43] R. Mélin, Ultralong-distance quantum correlations in three-terminal Josephson junctions, Phys. Rev. B **104**, 075402 (2021).

[44] See Supplemental Material at http://link.aps.org/supplemental/10.1103/PhysRevB.107.094505 for additional spectra of the driven Andreev molecule with varying coupling strengths to the reservoirs,and in the case of nonresonant dots. Information on the resonant structure of the resolvent and the treatment of oscillations at the Fermi scale is also given.

[45] D. R. Grempel, R. E. Prange, and S. Fishman, Quantum dynamics of a nonintegrable system, Phys. Rev. A **29**, 1639 (1984).

[46] N. Goldman and J. Dalibard, Periodically Driven Quantum Systems: Effective Hamiltonians and Engineered Gauge Fields, Phys. Rev. X **4**, 031027 (2014).

[47] M. Holthaus, Floquet engineering with quasienergy bands of periodically driven optical lattices, J. Phys. B: At., Mol. Opt. Phys. **49**, 013001 (2016).

[48] G. Casati and L. Molinari, Quantum chaos with time-periodic Hamiltonians, Prog. Theor. Phys. Suppl. **98**, 287 (1989).

[49] J. H. Shirley, Solution of the Schrödinger equation with a Hamiltonian periodic in time, Phys. Rev. **138**, B979 (1965).

[50] Y. B. Zel'Dovich, The quasienergy of a quantum-mechanical system subjected to a periodic action, ZhETF **51**, 1492 (1996) [Sov. Phys. JETP **24**, 1006 (1967)].

[51] H. Sambe, Steady states and quasienergies of a quantum-mechanical system in an oscillating field, Phys. Rev. A **7**, 2203 (1973).

[52] I. Martin, G. Refael, and B. Halperin, Topological Frequency Conversion in Strongly Driven Quantum Systems, Phys. Rev. X **7**, 041008 (2017).

[53] P. Coleman, *Introduction to Many-Body Physics* (Cambridge University Press, Cambridge, UK, 2015).

[54] V. Kornich, H. S. Barakov, and Y. V. Nazarov, Overlapping Andreev states in semiconducting nanowires: Competition of one-dimensional and three-dimensional propagation, Phys. Rev. B **101**, 195430 (2020).

[55] V. Benzoni, Hybridization of Andreev bound states in closely spaced Josephson junctions, Ph.D. thesis, Université Paris sciences et lettres, 2021, https://theses.hal.science/tel-03611001.

[56] K. S. Dy, S.-Y. Wu, and T. Spratlin, Exact solution for the resolvent matrix of a generalized tridiagonal Hamiltonian, Phys. Rev. B **20**, 4237 (1979).

[57] P. Giannozzi, G. Grosso, S. Moroni, and G. Pastori Parravicini, The ordinary and matrix continued fractions in the theoretical analysis of Hermitian and relaxation operators, Appl. Numer. Math. **4**, 273 (1988).

[58] S. Swain, Continued-fraction methods in atomic physics, *Advances in Atomic and Molecular Physics* Vol. 22 (Academic Press, New York, 1986), pp. 387–431.

[59] P. W. Anderson, Absence of diffusion in certain random lattices, Phys. Rev. **109**, 1492 (1958).

[60] J. Ziman, *Models of Disorder: The Theoretical Physics of Homogeneously Disordered Systems* (Cambridge University Press, Cambridge, UK, 1979).

[61] G. S. Uhrig, M. H. Kalthoff, and J. K. Freericks, Positivity of the Spectral Densities of Retarded Floquet Green Functions, Phys. Rev. Lett. **122**, 130604 (2019).

[62] J.-D. Pillet, Tunneling spectroscopy of the Andreev bound states in a carbon nanotube, Ph.D. thesis, Université Pierre et Marie Curie - Paris VI, 2011, https://tel.archives-ouvertes.fr/tel-00833472.

[63] A. Melo, C.-X. Liu, P. Rożek, T. Örn Rosdahl, and M. Wimmer, Conductance asymmetries in mesoscopic superconducting devices due to finite bias, SciPost Phys. **10**, 037 (2021).

[64] M. Houzet and P. Samuelsson, Multiple Andreev reflections in hybrid multiterminal junctions, Phys. Rev. B **82**, 060517(R) (2010).

[65] F. Setiawan and J. D. Sau, Electron-boson-interaction induced particle-hole symmetry breaking of conductance into subgap states in superconductors, Phys. Rev. Res. **3**, L032038 (2021).

[66] M. C. Toroker and U. Peskin, On the relation between steady-state currents and resonance states in molecular junctions, J. Phys. B: At., Mol. Opt. Phys. **42**, 044013 (2009).

[67] L. Dell'Anna, A. Zazunov, and R. Egger, Superconducting nonequilibrium transport through a weakly interacting quantum dot, Phys. Rev. B **77**, 104525 (2008).

[68] J. F. Rentrop, S. G. Jakobs, and V. Meden, Nonequilibrium transport through a Josephson quantum dot, Phys. Rev. B **89**, 235110 (2014).

[69] If M is the inverse of a block matrix

$$M = \begin{pmatrix} A & B \\ C & D \end{pmatrix}^{-1} = \begin{pmatrix} M_{11} & M_{12} \\ M_{21} & M_{22} \end{pmatrix}$$

then its upper-left block is equal to

$$M_{11} = (A - BD^{-1}C)^{-1}.$$

.